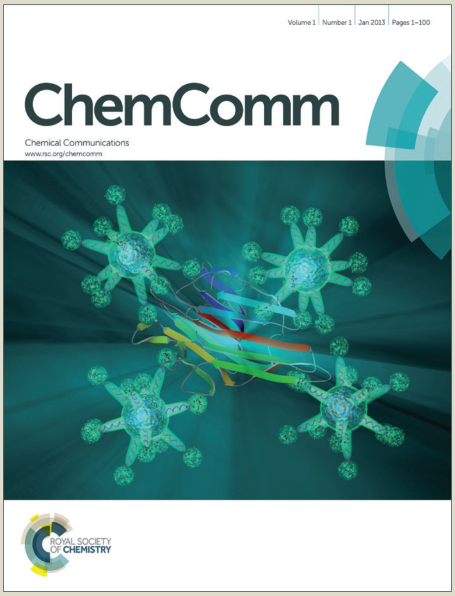
Volume 1 | Number 1 | Jan 2013 | Pages 1–100
ChemComm
Chemical Communications
www.rsc.org/chemcomm
ROYAL SOCIETY OF CHEMISTRY

ChemComm RSCPublishing

COMMUNICATION

Cite this: DOI: 10.1039/x0xx00000x

Tailoring metal–oxide interfaces of inverse catalysts of TiO_2/nanoporous-Au under hydrogen oxidation

Received 00th January 2015,

DOI: 10.1039/x0xx00000x

Kamran Qadir,[a,b] Bui Thi Phuong Quynh,[c] Hyosun Lee,[a,b] Song Yi Moon,[a,b] Sang Hoon Kim,[*,c] and Jeong Young Park[*,a,b]

Engineering metal–oxide interfaces in TiO_2/nanoporous (np) Au inverse catalysts results in enhancement of H_2 oxidation activity. While intrinsic activity of the novel np-Au prepared from a Au-Si alloy is low, the activity increased as the weight fraction of the TTIP (amount of TiO_2) was increased to 0.5 weight%. We correlate the change in activity with the active sites at the perimeter interface between the TiO_2 and np-Au.

Transition metal single crystals and supported nanoparticles utilizing two- and three-dimensional model catalytic systems have been extensively studied to investigate the molecular-scale origins of catalytic activity for heterogeneous oxidation reactions. Both ex situ and in situ investigations have helped to bridge the materials gap and identify the origins of such activity at atomic scales, including structural and electronic effects, surface oxide layers, and metal–oxide interfaces.[1–5] Among the transition metals, the intrinsic catalytic origin of Au is still controversial. Studies have shown that Au single crystals have an extremely low oxygen dissociation probability ($\ll 10^{-6}$) and weak interaction with most adsorbates. Since the activation of molecular oxygen is essential for oxidation catalysis, mechanistic studies relied on reactive oxygen sources, such as ozone or oxygen atoms.[6–8] Nonetheless, it was found that Au can be catalytically more active if dispersed as small particles (i.e., 2–5 nm) on a suitable oxide support, such as titania or ceria. Recent experiments on Au/TiO_2 as well as inverse TiO_2/Au catalysts have suggested that the enhanced catalytic activity can be ascribed to active sites at the TiO_2/Au interface.[9–12]

Recently, new novel unsupported nanoporous Au (np-Au) based materials have gained attention, which are prepared by leaching Ag, Cu, or Al from bimetallic Au alloys. The Au monolith consists of three-dimensional bicontinuous Au ligaments on the order of nanometres (10~50 nm), depending upon the preparation conditions. Such materials have been recently employed for catalyzing various gas-phase reactions, including low-temperature CO oxidation, H_2 oxidation, oxidative coupling of methanol, and partial oxidation of benzyl alcohol to benzaldehyde. The unsupported np-Au with less complexity can serve as a potential novel platform to address the intrinsic origin of the catalytic activity of Au-based catalysis.[13, 14] In Au catalysis, studies have suggested that undercoordinated atoms play a crucial role in the dissociation of O_2 molecules and that the support should be involved in supplying oxygen at the metal–oxide interface perimeter. For hydrogen dissociation, bulk Au is regarded as inactive, which is supported by quantum chemistry calculations;[15] however, hydrogen can be dissociated at low-coordinated edge or corner atoms on gold nanoparticles.[16] It is also suggested that both the shape and size of the gold particles are important for hydrogen dissociation.[17] In nanoporous Au, de-alloyed from Au-Ag or Au-Cu alloys, it is reported that undercoordinated surface atoms at the steps and kinks of Au ligaments are active sites. Additionally, residual Ag or Cu in such de-alloyed Au ligaments also contribute to improved catalytic performance. Despite a growing number of studies, the catalytic origins of Au-based catalysts are still debated.[18–20]

To address factors affecting the intrinsic activity of nanoporous Au, we investigated nanoporous Au de-alloyed from Au–Si instead of Ag or Cu. We varied the concentration of the Si in the Au_xSi_{1-x} alloy before dealloying, resulting in varying ligament diameters and porosities of the nanostructured Au. To generate the inverse metal oxide/np-Au structure, we deposited titania using liquid-phase deposition (i.e., immersion in a titanium tetraisoproproxide (TTIP) solution).We varied the amount of titania to engineer the metal–oxide interface and assess its role in altering catalytic activity. Hydrogen oxidation was carried out on all of the nanoporous Au catalysts, which served as a promising model reaction to address the catalytic origins of nanoporous Au. To investigate the intrinsic activity of the np-Au films, we prepared three different compositions of catalysts with varying porosity based on the amount of de-alloyed Si: np-Au-1, np-Au-2, and np-Au-3. The lowest amount of Si was in np-Au-1 while np-Au-3 had the highest amount. For np-Au-1, the roughness factor (i.e., (true surface area)/(geometric surface area)) value (RF) was 2.48, while np-Au-2 and np-Au-3 have higher RFs of 31.1 and 22.9, respectively, indicating that np-Au-1 has the lowest porosity while np-Au-2 exhibits the highest porosity. Fig. 1 shows representative field emission scanning electron microscope (FE-SEM) images of the three np-Au catalysts. As can be seen, each structure is comprised of interconnected Au ligaments, forming a bicontinuous porous network. Such Au ligaments are on the order of several nanometers. We selected the np-Au-2 film structure for fabrication of the TiO_2/np-Au inverse catalyst owing to its higher structural stability after the H_2 oxidation reaction and comparable activity under H_2 oxidation. The average ligament diameter of np-Au-2 was found to be 22.5 nm (Fig. 1b). The origin of the catalytic activity of np-Au is attributed to two factors: one is the low-coordinated Au atoms and the other is the residual metal species (Ag, Cu) in the np-Au.[13, 19, 20]

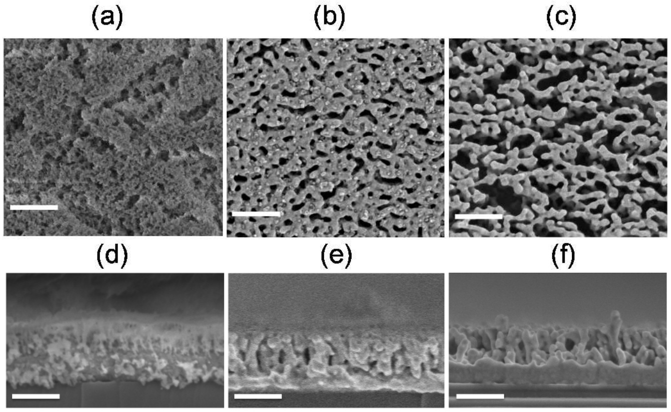

Fig. 1 Representative FE-SEM images of bare nanoporous Au films on a Si wafer. (a, b, c) Show top views and (d, e, f) show cross sectional views of np-Au-1, np-Au-2, and np-Au-3, respectively, with different levels of porosity based on the amount of de-alloyed Si in each catalyst. The resulting RFs of np-Au-1, np-Au-2, and np-Au-3 are 2.48, 31.1, and 22.89, respectively. The thickness of the nanoporous Au is ~ 150–200 nm (scale bar refers to 200 nm).

For Au catalysis, the activation of molecular oxygen is critical for oxidation reactions. It is believed that single-crystal Au surfaces have endothermic oxygen chemisorption energy, which implies that it does not bind oxygen and hence is considered inactive for oxidation catalysis.[21–23] Low-coordinated Au atoms are expected to interact more strongly with molecules due to their modified local and electronic structures that lead to a lower activation energy barrier and higher turnover frequency (TOF); therefore, they are regarded as the active sites in np-Au.[24, 25] Recently, a high density of atomic steps and kinks was observed on the curved surfaces of nanoporous Au, comparable to 3–5 nm nanoparticles,[19, 20] which are stabilized by hyperboloid-like gold ligaments. In situ environmental HR-TEM shows that surface reconstruction dynamics were suppressed for np-Au with increased Ag content, thus preserving a high density of atomic steps. The high catalytic activity of np-Au for catalyzing CO oxidation is attributed to a higher concentration of low-coordination atoms at these atomic steps. Catalytic activity is also attributed to residual Ag or Cu trapped inside the np-Au.[26–28] It is speculated that small quantities of Ag play a crucial role in the activation of molecular oxygen. Compared with gold, molecular oxygen tends to bind strongly to Ag and is, therefore, more easily activated. Wittstock et al. found that in situ XPS reveals that Ag is present at the surface of np-Au in significant amounts and its chemical state undergoes major changes when exposed to reactive gas conditions (e.g., a mixture of O_2 and CO at ~ 1 mbar).[18] It was also reported that residual Ag contributes to catalytic activity by stabilizing the atomic steps and suppressing faceting kinetics.[20] Kameoka et al. reported that np-Au prepared by dealloying intermetallic $AuCu_3$ compounds also exhibits some activity towards CO oxidation, even in the absence of Ag.[29] The majority of these studies have utilized np-Au prepared by dealloying Au–Ag monoliths,[13] we focused on preparing and investigating Au catalysts without any residual elements (such as Ag and Cu) to assess the activity of np-Au[30] under the H_2 oxidation reaction. However it is now well established that highly active Au catalysts are comprised of small Au nanoparticles supported on a porous metal oxide, such as titania or ceria, and that the perimeter interface provides active sites.[31–36] In addition to a high dispersion of nanoparticles, the support is considered critical for catalytic activity, as pure Au lacks high activity towards molecular oxygen dissociation.[37] Along with the debate about the catalytic activity of low-coordinated Au atoms, it is speculated that the support is involved in supplying oxygen (e.g., at the particle perimeter).[38, 39] Recently, Green et al. reported that the interface between the Au support and the metal oxide particle not only serves as common adsorption sites for reactant molecules, such as CO, but also enables efficient activation of molecular oxygen. They observed dual catalytic sites along the perimeter of 3 nm Au nanoparticles supported on titania during CO oxidation.[40]

To elucidate the role of the interface between the Au and oxide, we deposited titania on np-Au and controlled its thickness and coverage by depositing varying amounts of titania (see Fig. 2). Titania was deposited using liquid-phase immersion deposition with a TTIP solution in ethanol using 0.1, 0.5, and 1 weight% TTIP. To assess the Au–TiO_2 interfacial structure and its effect on the nature of the active sites in the catalytic activity of H_2 oxidation, we investigated the cross-sectional interface of titania deposited on np-Au ligaments (prepared using FIB milling) under TEM to identify the nature of the deposited titania.

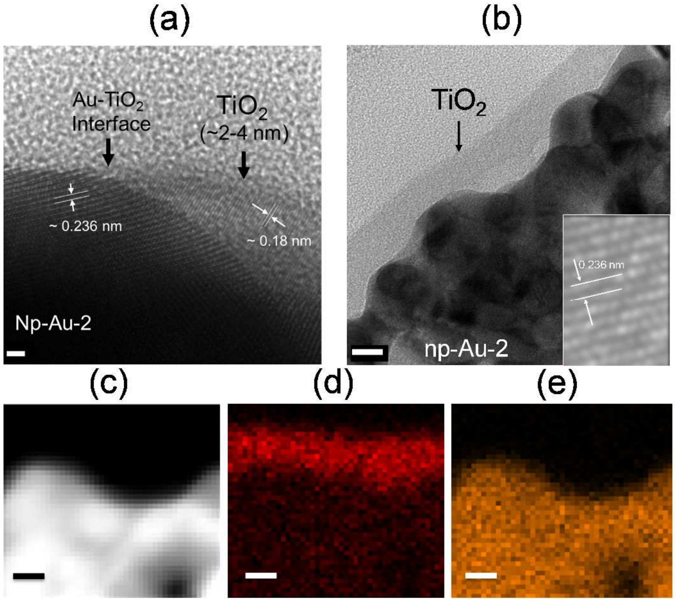

Fig. 2 HR-TEM investigation of TiO_2/np-Au catalysts. (a) Shows a cross-sectional HR-TEM image of the 0.1 weight% TTIP-impregnated TiO_2/np-Au catalyst showing the lattice images of Au and TiO_2 (scale bar refers to 1 nm). (b) Shows a cross-sectional HR-TEM image of the 1.0 weight% TTIP-impregnated TiO_2/np-Au film catalyst. The inset shows a lattice image of the Au (scale bar refers to 2 nm). (c, d, e) Show corresponding HAADF-STEM-EDS mapping images of the 1.0 weight% TTIP-impregnated np-Au catalyst. It shows that the titania layer is largely deposited on the outer peripheral area of the nanoporous Au ligament surface (scale bars refer to 10 nm).

Fig. 2 shows cross-sectional high-resolution transmission electron microscope (HR-TEM) images of the TiO_2/np-Au-2 catalysts. Fig. 2a shows a cross section of TiO_2/np-Au-2 prepared by immersion in the 0.1 weight% TTIP precursor solution. The cross section clearly shows the interface between the Au and TiO_2 (see also Fig. S1 in the ESI). Fig. 2b shows cross-sectional HR-TEM images of the 1.0 weight% TTIP-based TiO_2/np-Au catalyst. Here the thickness of the titania layer is ~15 nm, and the inset shows a high-resolution TEM image of the Au lattice. To investigate the deposition depth of the titania from immersion of the np-Au catalysts in the TTIP precursor solution, we carried out EDS mapping of the Ti and Au. As can be seen in Fig. 2c–e, the high-angle annular dark field scanning transmission electron microscopy energy-dispersive X-ray spectroscopy (HAADF-STEM-EDS) mapping images of the

TiO_2/np-Au catalysts prepared using 1.0 weight% TTIP, the titania layer largely forms on the top surface. Therefore, we expect that such a titania layer terminates on the outer peripheral area of the Au ligaments and does not form inside the bicontinuous Au skeleton. The Au–TiO_2 perimeter area therefore lies at such termination boundaries and are probable active perimeter sites during catalytic H_2 oxidation. Structural information for the TiO_2/np-Au was also shown in the XRD patterns (see Fig. S2 in the ESI). After deposition of titania on the np-Au films, we checked the surface oxidation state and/or composition of the catalysts using XPS. The reason was two-fold: one was to confirm the nature of the deposited titania (i.e., oxidation state), and the second was to assess the surface oxidation states of the Au. (Fig. S3 in the ESI summarizes the XPS oxidation states for all of the TiO_2/np-Au systems).

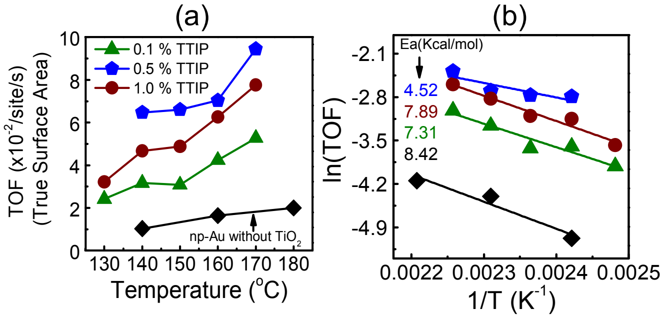

Fig. 3 Catalytic activity of H_2 oxidation on TiO_2/np-Au catalysts: (a) turnover frequency as a function of temperature and (b) Arrhenius plots and activation energies (Ea) in kcal/mol. Compared to bare nanoporous Au, the TOF is enhanced after TiO_2 deposition via TTIP impregnation.

Fig. 3a shows the turnover frequency for the TiO_2/np-Au catalysts. Fig. 3b shows the corresponding Arrhenius plots. It is observed that, compared with bare np-Au, the activity is enhanced after deposition of TiO_2. The TOF varies depending upon the concentration and thickness/coverage of the deposited titania, as confirmed by the HR-TEM cross-sectional images. The activity is lowest for the 0.1 weight% TTIP precursor, while it is highest for the 0.5 weight% TTIP precursor. The increase in concentration of the TTIP precursor to 1 weight% TTIP leads to a reduction of the catalytic activity. The reduction in catalytic activity suggests a corresponding decrease in active TiO_2/np-Au perimeter sites due to the higher surface coverage. The activation energies for the TiO_2/np-Au catalysts were obtained from Arrhenius plots of the catalytic activity (Fig. 3b). We found that bare np-Au has the highest activation energy (Ea) of 8.42 kcal/mol. The Ea is lowest for 0.5 weight% TTIP-loaded np-Au (i.e. 4.52 kcal/mol), indicating the active nature of the catalyst. We also found that the morphology of all of the TiO_2/np-Au catalysts were preserved after H_2 oxidation (see Fig. S4 in the ESI). Additionally, the turnover frequencies were measured on the TiO_2/np-Au over several hours (See Fig. S5 in the ESI), exhibiting the absence of deactivation.

What is the role of the perimeter interface in exhibiting a higher TOF on our TiO_2/np-Au inverse catalysts during catalytic H_2 oxidation? Fujitani et al.[9] found that the H_2–D_2 exchange reaction did not take place on single crystal surfaces of Au (111), Au (311), and TiO_2 (110), but it proceeded smoothly on Au/TiO_2 (110) surfaces with different sizes of Au nanoparticles (NPs), implying that H_2 dissociation sites are available. In the case of Au NPs on TiO_2 (110), they found that the HD formation rate increased sharply when the Au particle size was below 2 nm, whereas the turnover frequency (based on the length of the perimeter interfaces between the Au NPs and TiO_2 (110)) remained almost constant irrespective of the Au particle size. They suggested that active sites for H_2 dissociation are located at the periphery around the Au NPs attached to TiO_2 and that the catalytic activity for H_2 dissociation is neither correlated to a change in the fraction of edge or corner sites nor to a change in the electronic nature induced by the quantum size effect. We believe that the increase in TOF for the TiO_2/np-Au system can be correlated to the availability of such H_2 dissociation Au sites at the termination boundaries of the TiO_2 over the np-Au ligaments. Furthermore, Nakamura et al.[10] found that HD was produced only over the Au (111) surface bearing stoichiometric TiO_2. They found a proportional relationship between the HD formation rate and TiO_2 concentration, implying that the amount of stoichiometric TiO_2 is essential for the creation of hydrogen dissociation sites on Au in contact with TiO_2. This is in agreement with our XPS observations of the TiO_2/np-Au-2 catalyst that show stoichiometric TiO_2 formation (Fig. S3 in the ESI). Green et al. reported H_2 oxidation over Au/TiO_2 powder catalysts synthesized using the deposition precipitation method.[41] They proposed dual perimeter active sites (Au perimeter site and TiO_2 perimeter site that operate together during catalytic reactions) based on kinetic analysis utilizing in situ infrared spectroscopy and density functional theory calculations. They observed atomic hydrogen spillover from supported Au nanoparticles over TiO_2 surfaces based on an upward shift in the infrared background. No products were formed over the pure TiO_2 catalyst, whereas H_2O formation occurred on the Au/TiO_2.

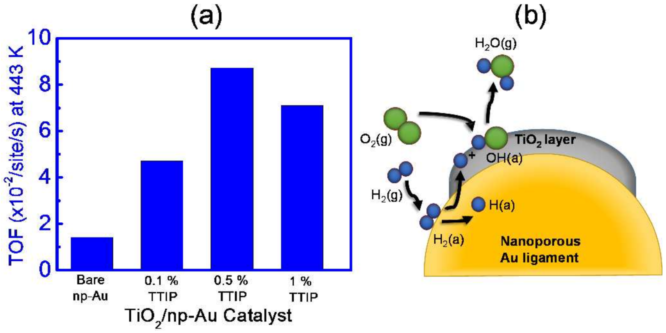

Fig. 4 (a) Summary of the TOF for all TiO_2/np-Au catalysts at 443 K under H_2 oxidation. The TOF increased 4-fold for the 0.5 weight% TTIP-impregnated TiO_2/np-Au catalysts in relation to the bare np-Au film. (b) A schematic representation of catalytic H_2 oxidation at the TiO_2/np-Au perimeter interface created between the nanoporous Au ligament and the deposited titania layers. Hydrogen molecules adsorb on the np-Au perimeter sites, followed by dissociation and spilling to the titania; gaseous O_2 molecules adsorbing on the titania perimeter sites form Ti-OOH species that dissociate into Ti-O and Ti-OH species. The Ti-OH species finally hydrogenate to form H_2O molecules.

The higher TOF of the np-Au after stoichiometric TiO_2 deposition suggests that the perimeter Au sites are more active at the TiO_2–Au interface. Additionally, the TOF dependence on TiO_2 concentration can be attributed to a variation in the number of such active sites, which in turn can tune the catalytic activity during H_2 oxidation. Fig. 4a summarizes the TOF results for all of the TiO_2/np-Au catalysts at 443 K to elucidate the importance of the TiO_2/np-Au composite system, compared with bare np-Au catalysts. The activities of the inverse catalysts show the highest enhancement when using 0.5 weight% TTIP, resulting in a 4-fold increase in TOF.

Green et al.[41] showed that during H_2 oxidation, dual parameter sites that comprise Ti5c sites (coordination number (CN) = 5) and a neighbouring Au perimeter site (CN = 7) are the most favoured of all sites since O_2 adsorption at the Ti5c perimeter site lowers the barrier for the dissociative adsorption of gaseous H_2 at the neighboring Au perimeter site down to 0.16 eV. A dual parameter site thus produces Ti-OOH and Au-H surface intermediates. The Ti-OOH species dissociate into Ti-OH and Ti-O species (dissociation barrier (Ea) = 0.20 eV). The reaction proceeds via hydrogenation of two Ti-OH species by Au-H species to form H_2O molecules. Fig. 4b shows the proposed reaction mechanism during catalytic H_2 oxidation at the TiO_2/np-Au-2 perimeter interface based on hydrogen atoms spilling to the titania and the final hydrogenation of the Ti-OH species by Au-H. Since bare nanoporous Au also exhibits negligible catalytic activity and is not inert during H_2 oxidation, it implies that other reaction mechanisms exist in addition to the proposed one. We suggest such activity can be correlated to the activation of H_2 and O_2 at the low-coordinated Au atoms along steps and edges at the concave/convex curvatures of the nonporous Au (analogous to Au nanoparticles).[15, 19, 20]

Conclusions

In conclusion, we found that intrinsic H_2 oxidation activity of np-Au catalysts prepared by de-alloying Au-Si was low for bare np-Au. The activity increased after titania deposition for all catalysts. This implies that the TiO_2–Au interface provides active sites resulting in higher TOFs for H_2O formation. We show that the TiO_2–Au interface sites can be modified to tune the catalytic activity depending on the concentration of the titania layer. This approach shows a promising route to design catalysts with tuneable properties for various technological applications.

Acknowledgements

This work was supported by the Institute for Basic Science (IBS-R004-G4), Republic of Korea, and by a grant from the future R&D Program funded by KIST (2E24610) and the KUUC (KIST-UNIST Ulsan Centre for Convergent Materials) Centre (2V03280).

Notes and references

[a] Center for Nanomaterials and Chemical Reactions, Institute for Basic Science, Daejeon, 305-701, Republic of Korea.
[b] Graduate School of EEWS, Korea Advanced Institute of Science and Technology (KAIST), Daejeon , 305-701 , Republic of Korea.
[c] Center for Materials Architecturing, Korea Institute of Science and Technology (KIST), Seoul, 136-791, Republic of Korea.

†Electronic Supplementary Information (ESI) available: [Experimental data including HR-TEM (Fig. S1), XRD patterns (Fig. S2) and XPS of TiO_2/np-Au (Fig. S3), FE-SEM images of TiO_2/np-Au before and after H_2 oxidation (Fig. S4) and turnover number of H_2O molecules with time (Fig. S5). See DOI: 10.1039/b000000x/

1. G. A. Somorjai, R. L. York, D. Butcher and J. Y. Park, *Physical Chemistry Chemical Physics*, 2007, **9**, 3500-3513.
2. J. Y. Park, *Current Trends of Surface Science and Catalysis*, Springer New York, 2013.
3. K. Qadir, S. H. Joo, B. S. Mun, D. R. Butcher, J. R. Renzas, F. Aksoy, Z. Liu, G. A. Somorjai and J. Y. Park, *Nano Letters*, 2012, **12**, 5761-5768.
4. K. Qadir, S. M. Kim, H. Seo, B. S. Mun, F. A. Akgul, Z. Liu and J. Y. Park, *The Journal of Physical Chemistry C*, 2013, **117**, 13108-13113.
5. K. Qadir, S. H. Kim, S. M. Kim, H. Ha and J. Y. Park, *The Journal of Physical Chemistry C*, 2012, **116**, 24054-24059.
6. B. Xu, X. Liu, J. Haubrich, R. J. Madix and C. M. Friend, *Angewandte Chemie International Edition*, 2009, **48**, 4206-4209.
7. X. Liu, B. Xu, J. Haubrich, R. J. Madix and C. M. Friend, *Journal of the American Chemical Society*, 2009, **131**, 5757-5759.
8. J. Gong, D. W. Flaherty, R. A. Ojifinni, J. M. White and C. B. Mullins, *The Journal of Physical Chemistry C*, 2008, **112**, 5501-5509.
9. T. Fujitani, I. Nakamura, T. Akita, M. Okumura and M. Haruta, *Angewandte Chemie International Edition*, 2009, **48**, 9515-9518.
10. I. Nakamura, H. Mantoku, T. Furukawa and T. Fujitani, *The Journal of Physical Chemistry C*, 2011, **115**, 16074-16080.
11. D. A. Panayotov and J. T. Yates, *The Journal of Physical Chemistry C*, 2007, **111**, 2959-2964.
12. I. X. Green, W. Tang, M. Neurock and J. T. Yates, *Angewandte Chemie International Edition*, 2011, **50**, 10186-10189.
13. A. Wittstock, A. Wichmann and M. Bäumer, *ACS Catalysis*, 2012, **2**, 2199-2215.
14. T. Déronzier, F. Morfin, L. Massin, M. Lomello and J.-L. Rousset, *Chemistry of Materials*, 2011, **23**, 5287-5289.
15. B. Hammer and J. K. Norskov, *Nature*, 1995, **376**, 238-240.
16. E. Bus, J. T. Miller and J. A. van Bokhoven, *The Journal of Physical Chemistry B*, 2005, **109**, 14581-14587.
17. C. Mohr, H. Hofmeister, J. Radnik and P. Claus, *Journal of the American Chemical Society*, 2003, **125**, 1905-1911.
18. A. Wittstock, B. Neumann, A. Schaefer, K. Dumbuya, C. Kübel, M. M. Biener, V. Zielasek, H.-P. Steinrück, J. M. Gottfried, J. Biener, A. Hamza and M. Bäumer, *The Journal of Physical Chemistry C*, 2009, **113**, 5593-5600.
19. T. Fujita, P. Guan, K. McKenna, X. Lang, A. Hirata, L. Zhang, T. Tokunaga, S. Arai, Y. Yamamoto, N. Tanaka, Y. Ishikawa, N. Asao, Y. Yamamoto, J. Erlebacher and M. Chen, *Nature Materials*, 2012, **11**, 775-780.
20. T. Fujita, T. Tokunaga, L. Zhang, D. Li, L. Chen, S. Arai, Y. Yamamoto, A. Hirata, N. Tanaka, Y. Ding and M. Chen, *Nano Letters*, 2014, **14**, 1172-1177.
21. J. K. Norskov, T. Bligaard, B. Hvolbaek, F. Abild-Pedersen, I. Chorkendorff and C. H. Christensen, *Chemical Society Reviews*, 2008, **37**, 2163-2171.
22. X. Zhang and Y. Ding, *Catalysis Science & Technology*, 2013, **3**, 2862-2868.
23. B. Hvolbæk, T. V. W. Janssens, B. S. Clausen, H. Falsig, C. H. Christensen and J. K. Nørskov, *Nano Today*, 2007, **2**, 14-18.
24. H. Falsig, B. Hvolbæk, I. S. Kristensen, T. Jiang, T. Bligaard, C. H. Christensen and J. K. Nørskov, *Angewandte Chemie International Edition*, 2008, **47**, 4835-4839.
25. C. Lemire, R. Meyer, S. Shaikhutdinov and H.-J. Freund, *Angewandte Chemie International Edition*, 2004, **43**, 118-121.
26. E. Seker, M. L. Reed and M. R. Begley, *Materials*, 2009, **2**, 2188-2215.
27. A. Wittstock, B. Neumann, A. Schaefer, K. Dumbuya, C. Kuebel, M. M. Biener, V. Zielasek, H.-P. Steinrueck, J. M. Gottfried, J. Biener, A. Hamza and M. Baeumer, *Journal of Physical Chemistry C*, 2009, **113**, 5593-5600.
28. Y. Ding and M. Chen, *Mrs Bulletin*, 2009, **34**, 569-576.
29. S. Kameoka and A. Tsai, *Catalysis letters*, 2008, **121**, 337-341.
30. B. T. P. Quynh, J. Y. Byun and S. H. Kim, *Sensors and Actuators B: Chemical*, 2014, **193**, 1-9.
31. A. Schaefer, D. Ragazzon, L. E. Walle, M. H. Farstad, A. Wichmann, M. Bäumer, A. Borg and A. Sandell, *Applied Surface Science*, 2013, **282**, 439-443.
32. A. Kudo, T. Fujita, X. Lang, L. Chen and M. Chen, *MATERIALS TRANSACTIONS*, 2010, **51**, 1566-1569.
33. C. Jia, H. Yin, H. Ma, R. Wang, X. Ge, A. Zhou, X. Xu and Y. Ding, *The Journal of Physical Chemistry C*, 2009, **113**, 16138-16143.
34. M. Haruta, *Catalysis Today*, 1997, **36**, 153-166.
35. M. Kotobuki, R. Leppelt, D. A. Hansgen, D. Widmann and R. J. Behm, *Journal of Catalysis*, 2009, **264**, 67-76.
36. Z. Zhou, S. Kooi, M. Flytzani-Stephanopoulos and H. Saltsburg, *Advanced Functional Materials*, 2008, **18**, 2801-2807.
37. J. M. Gottfried, K. J. Schmidt, S. L. M. Schroeder and K. Christmann, *Surface Science*, 2003, **525**, 184-196.
38. G. C. Bond and D. T. Thompson, *Catalysis Reviews*, 1999, **41**, 319-388.
39. G. Bond and D. Thompson, *Gold Bull.*, 2000, **33**, 41-50.
40. I. X. Green, W. Tang, M. Neurock and J. T. Yates, *Science*, 2011, **333**, 736-739.
41. I. X. Green, W. Tang, M. Neurock and J. T. Yates, Jr., *Angewandte Chemie-International Edition*, 2011, **50**, 10186-10189.

Table of Contents

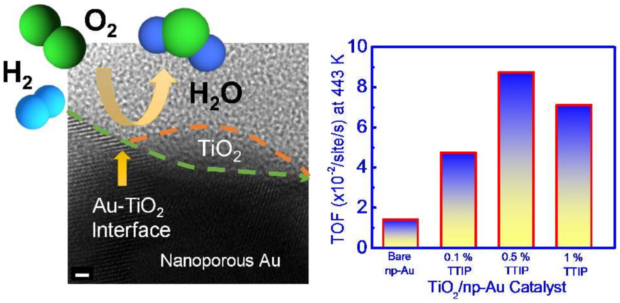

Catalytic activity of nanoporous Au prepared from a Au-Si alloy is enhanced by engineering Au–TiO$_2$ interfaces under H$_2$ oxidation